land

MDPI

Article

Forecasting of Wildfire Probability Occurrence: Case Study of a Mediterranean Island of Italy

Davide Berardi, Marta Galuppi *, Angelo Libertà and Mara Lombardi

Department of Chemical Engineering Materials Environment (DICMA), Sapienza-University of Rome, via Eudossiana 18, 00184 Rome, Italy; davide.berardi@uniroma1.it (D.B.); angelo.liberta@uniroma1.it (A.L.); mara.lombardi@uniroma1.it (M.L.)

* Correspondence: marta.galuppi@uniroma1.it

Abstract: The growing need to address natural and human-induced disasters while protecting territory remains a key focus for the scientific community. Effective emergency management, especially during wildfires, requires coordinated responses to safeguard lives and assets. This study develops hazard maps to aid emergency planning in Italy and estimate territorial resilience indicators. Focusing on wildfire ignition hazards in Ischia, the study uses a probabilistic model based on fifteen years of wildfire data (2009–2023). By analyzing ignition points and employing a Poisson distribution, it correlates ignition probabilities with vegetation types. The hazard maps reveal that wildfire risk is primarily influenced by the wildland–urban interface and vegetation characteristics, emphasizing the need to integrate territorial and urban factors into wildfire forecasting. The findings also suggest areas for refining the model to enhance risk mitigation strategies.

Keywords: ignition points; wildfire forecasting; wildland–urban interface; vulnerability assessment; spatial distribution; fire resilience

check for updates

Academic Editor: Nikos Koutsias

Received: 6 December 2024
Revised: 17 January 2025
Accepted: 28 January 2025
Published: 29 January 2025

Citation: Berardi, D.; Galuppi, M.; Libertà, A.; Lombardi, M. Forecasting of Wildfire Probability Occurrence: Case Study of a Mediterranean Island of Italy. *Land* **2025**, *14*, 277. https://doi.org/10.3390/land14020277

Copyright: © 2025 by the authors. Licensee MDPI, Basel, Switzerland. This article is an open access article distributed under the terms and conditions of the Creative Commons Attribution (CC BY) license (https://creativecommons.org/licenses/by/4.0/).

1. Introduction

Predicting wildfire behavior and spread remains one of the greatest challenges for current management programs aimed at developing strategies for restoring affected areas [1]. Fires, an integral part of social and ecological systems, require innovative techniques for more effective management. The increase in the number and devastating effects of fires, exacerbated by climate change and vegetation alterations [2–4], has made proactive actions and new strategies for wildfire risk management essential.

As a result, there is broad interest among the scientific community regarding the necessity to focus more attention on modeling the behavior and spread dynamics of wildfires [5]. It is now well-known that, in addition to posing a potential threat to ecosystems and urban–rural interface areas [6], wildfires can also cause alterations to the soil and the microorganisms within it. Fire suppression efforts are significantly aided by road access, which suggests, like the findings of Ager et al. [7], that the likelihood of a large fire increases with distance from roads. This could partly be attributed to reduced suppression efficiency in those more remote areas. As wildfire management strategies, also identification of notable differences in pine regeneration, overall plant cover, and plant community composition based on pre-fire treatments suggests that, while fire severity remains the primary factor influencing vegetation changes, pre-fire treatments can still affect post-fire plant communities [8].

Traditionally, wildfire modeling and study were based on engineering and fire safety, control strategies, as well as the emissions of smoke and pollutants, damaging the air

quality [9], into the atmosphere. However, given the increasing frequency and extent of wildfires affecting ever-wider natural areas, leading to substantial alterations in hydrological and ecological processes, it is now essential to consider the territory's response, including recovery times and the evolution of post-fire soil conditions [10]. Numerous studies, for example, the research conducted by Borja et al. [11], indicate that over the long term, the impact of hillslope stabilization techniques on vegetation regeneration gradually decreases across nearly all soil properties and ground covers. Depending on temperature and duration, the degradation, pyrolysis, and combustion of carbon can lead to soil structure breakdown, altering its infiltration capacity, increasing erosion rates, and making it more susceptible to dangerous debris flows and landslides [12,13]. Therefore, the development of new tools that allow for the prediction and anticipation of wildfire spread is crucial for outlining specific prevention and planning programs. This prediction model could be based on mathematical and mechanical parameters [14,15], machine learning techniques, such as neural networks trained on databases [16] or agent-based models which are largely applied to wildfire event management [17].

In this context, the secondary effects related to wildfires are becoming increasingly central to the design of more resilient infrastructure systems capable of functioning effectively in complex environments subject to multiple hazards [18]. There is an urgent need to shift towards more resilient policies that effectively address fire-related issues while ensuring long-term sustainability, as shown by Arango et al. [19]. This shift does not mean reducing efforts in wildfire suppression but emphasizes the need for greater focus and investment in areas like prevention and protection [20] and especially in the field of wildfire evacuation [21].

Studies performed over the last decade quantify the dynamic interactions characterizing these phenomena, and it is becoming evident that without considering the dynamic complexity of natural disasters, impact assessments tend to underestimate risk and provide misleading information regarding emergency management priorities and planning [22,23]. Small disturbances in a single system could trigger a series of cascading failures in other systems, thereby inducing further damage to other infrastructures.

Wildfire risk is addressed through multiple approaches, with some focusing on correlating the phenomenon with predisposing factors, while others aim to define metrics for predictive models to support risk management. In Europe, wildfire risk assessment typically considers the medium and long-term effects on the territory, recognizing the potential to trigger or exacerbate other natural events in areas already vulnerable to specific conditions. For instance, in Bulgaria, Borisova et al. [24] propose a flexible, location-specific framework for assessing and mapping wildfire risk, particularly in the context of natural heritage and resource management. This framework integrates 29 indicators across five thematic groups—covering hazards, vulnerability, and emergency response—and evaluates risk at the forestry subdivision level, the smallest unit of forest management. Geospatial technologies are employed to analyze data and generate risk maps.

In France, Caron et al. [25] introduce a novel probability analysis method in the preprocessing stage to predict wildfires, focusing on rare events. The study, based on wildfire data from several French departments between 2015–2022, utilizes a calibrated regression model to predict the probability of at least one fire occurring on a given day. This model distinguishes itself by incorporating fires of all sizes and causes, rather than focusing on large-scale fires, and demonstrates a balanced approach between log loss and Expected Calibration Error.

In Spain, Liz-López et al. [26] present the Wildfire Assessment Model (WAM), a deep learning-based method designed to predict the economic and ecological impacts of wildfires in regions such as Castilla y León and Andalucía. The WAM utilizes a residual-style

convolutional network to assess atmospheric variables and the greenness index, estimating resources needed, control and extinction time, and expected burned area. The model is pre-trained with 100,000 examples of unlabeled data and fine-tuned with a smaller dataset of 445 samples. This pretraining improves the model's ability to predict wildfire scenarios, offering enhancements over baseline models and demonstrating practical applications through regional assessment maps.

In Italy, where wildfires exhibit a significant seasonal pattern, Arima et al. [27] propose a Poisson model for zero-inflated spatial counts, addressing measurement error, excess zeroes, and spatial dependencies. Bayesian inference is applied using MCMC through the R package NIMBLE. The model is tested using MODIS satellite data from two neighboring Italian regions during the summer of 2021, incorporating socio-economic and environmental risk factors. The results indicate the model's effectiveness in analyzing wildfire occurrences and providing valuable insights into spatial risk patterns.

In the United States, Keeping et al. [28] developed a new model for predicting the daily probability of wildfire occurrence at approximately 10 km spatial resolution using a generalized linear modeling (GLM) approach. This model incorporates improvements in variable selection, predictor range identification, and compression minimization through an ensemble of model runs. It successfully predicts geospatial fire patterns, interannual variability, and regional seasonal cycles.

Gonzalez-Mathiesen et al. [29] explore the challenges of integrating wildfire information into spatial planning processes in Victoria (Australia) and Chile. The study identifies key elements that hinder the development of effective wildfire risk management, including identification, co-generation, reframing, and implementation. It finds that these planning systems often fail to incorporate dynamic wildfire data, limiting the potential for improving resilience to wildfires.

Finally, Wei et al. [30] apply the Convolutional Non-homogeneous Poisson Process (cNHPP) model to quantify wildfire ignition risks on power delivery networks. Unlike traditional fire danger indices, the cNHPP model accounts for both instantaneous and cumulative environmental factors, as well as spatial–temporal dependencies across network segments. This model is applied to major transmission lines in California, using historical fire, meteorological, and vegetation data to estimate wildfire risks.

This study presents a comprehensive investigation into wildfire occurrence probability on the island of Ischia, Italy, focusing on the identification of ignition points, the determination of wildfire causes, and the hazard assessment across different land cover classes. The article is organized as follows. The introduction outlines the research objectives and perspectives. Section 2 describes the materials and methods, including the mathematical models and key considerations. Section 3 presents the results of the wildfire ignition modeling, while Section 4 provides a discussion of these findings and their limitations. Finally, Section 5 concludes the study and outlines future research directions.

2. Materials and Methods

The objective of this study is to deepen the understanding of the spatial and temporal patterns of wildfires and to contribute to the development of effective risk mitigation strategies through hazard maps. Figure 1 illustrates the workflow used to achieve this objective. The model integrates the analysis of available ignition point data, statistical modeling to assess the likelihood of wildfire ignition, and hazard mapping to identify high-risk areas. This approach enables the development of targeted strategies to mitigate the impacts of wildfires and supports better-informed decision-making in wildfire management and land-use planning.

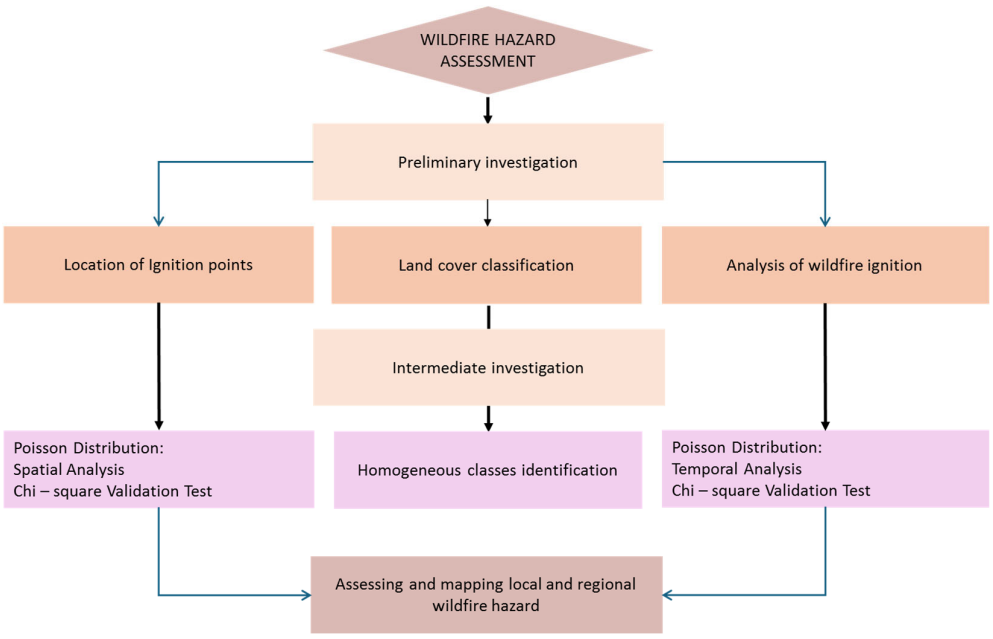

Figure 1. Flow chart of the model procedure for estimating wildfire ignition probability.

The research was structured in several phases to systematically address the study's objectives. The initial phase involved a preliminary investigation into the location of ignition points on the island of Ischia. Field data, combined with satellite imagery, were used to precisely map the historical locations of wildfire occurrences. This step was pivotal for detecting patterns in the spatial distribution of wildfires across different land cover types, providing a basis for further analysis and understanding of risk factors related to specific vegetation characteristics.

An analysis of wildfire ignition causes (2009–2023) was subsequently conducted. By examining weather data, human activities, and environmental factors, the study identified both anthropogenic and natural ignition triggers. Although this extended observation period is not usually considered long-term in seasonal trend analysis, it allowed for the identification of extended patterns and seasonal variations in wildfire occurrences. This provided valuable insights into the recurring conditions that contribute to wildfire risk. Next, the island's cover land was categorized into homogeneous classes based on the identified ignition points. These classes were defined by land use patterns, vegetation types, and topographical features. This classification was designed to streamline the analysis by grouping areas with comparable fire risk factors, enabling hazard estimation and subsequent risk mapping. This method supports targeted wildfire risk assessment in regions with analogous environmental and structural characteristics, improving the precision and applicability of the study's findings.

Following Papakosta et al. [31] the study developed a probabilistic wildfire prediction model using the Poisson distribution, based on readily available spatial–temporal datasets to enhance their operational applicability. Critical variables influencing the predictions include meteorological conditions, land cover types, and indicators of human activity. That is, a Poisson distribution model was applied to estimate the likelihood of wildfire occurrences within each land cover class. This model, suitable for critical event analysis, was integrated with spatiotemporal analysis to incorporate both geographic and temporal aspects of ignition points. Additionally, a chi-square test was conducted to validate the model hypothesis and confirm the reliability of the results. The test was used to verify whether the observed frequencies of ignition fires over a fifteen-year period (from 2009 to 2023) [32] in one or more categories matched the expected frequencies. This step aims to

assess the significance of the observed patterns and the accuracy of land cover classifications. The chi-square test results reinforced the robustness of the Poisson distribution model in predicting wildfire occurrences across different land cover types.

Finally, the study estimated both local and regional wildfire hazards for land cover classes. Local hazard estimates provided detailed insights into the specific risk levels across distinct regions of the island, while the regional hazard estimation offered a comprehensive overview of wildfire risk for Ischia as a whole. These findings are expected to inform future land management and fire prevention strategies, and evidence-based decision-making to mitigate wildfire risk effectively.

2.1. Preliminary Investigation of the Location of Ignition Points

To estimate fire propensity and thus determine the hazard level of the representative area, a preliminary analysis was conducted involving the collection of data on past wildfire events over a defined observation period. This included identifying the representative vegetation species related to the ignition points. The research targeted wildfires that occurred from 2009 to 2023, encompassing the last fifteen years of monitoring activity. Data were sourced from the Campania region geoportal and the wildfire register, which provided access to historical records detailing the perimeters of fire-affected areas. These records, maintained by the Forest command of the Carabinieri of the Campania region, were essential for accurately mapping past wildfire occurrences and analyzing vegetation types associated with ignition points [32]. Between 2009 and 2023, approximately 132 wildfires were recorded on the island of Ischia, affecting an estimated 265 hectares in total. To facilitate deeper analysis and structure the subsequent phases of research, each wildfire incident was systematically categorized according to specific parameters, including:

- year of occurrence: enabling an understanding of annual variations and potential trends over the observation period;
- fire identifier: a unique reference code for each incident, ensuring precise tracking and reference in datasets;
- fire date: capturing the exact timing of each incident to help identify seasonal or weather-related patterns;
- location and area burned: specifying the geographic location and the size of each affected area to allow for spatial analysis in relation to land cover types, vegetation, and proximity to urban zones.

This classification framework lays the groundwork for detailed statistical modeling, allowing for a classification of the underlying factors influencing wildfire occurrence and facilitating targeted hazard assessments.

An initial comparative analysis found that from the total of the 132 wildfires recorded over the observation period, 90 incidents occurred during the peak wildfire suppression campaign period (15 June–30 September), with the remaining 42 fires occurring sporadically across other months. Following this categorization, the next step involved integrating shapefiles that provided the exact locations of each ignition point. These spatial data were essential for assessing the characteristics of the surrounding terrain and vegetation. Due to data limitations, it was necessary to manually reconstruct the perimeter of each fire using AutoCAD software 2025 [33], followed by their georeferencing in QGIS 3.38 [34], as depicted in Figure 2.

After the step of the georeferencing for recorded fires, the next phase focused on combining the gathered data with thematic maps available in QGIS [34]. This step aimed to pinpoint the precise location of ignition points and required integrating various spatial data layers to capture relevant environmental and geographic details. This process

utilized essential information derived from both raster and vector layers, covering the following categories:

- Vegetation, land use, and land cover: it provided insight into the type and distribution of vegetation, which is critical for assessing fire risk based on fuel availability.
- Perimeters and urban areas: it offered a spatial reference for fire perimeters and proximity to urban areas, important for understanding potential risks to human infrastructure.
- Road and trail networks: these layers helped identify access routes, essential for evaluating potential fire spread and planning for suppression logistics.
- Local meteorological data: climate factors, such as temperature, humidity, and wind patterns, were incorporated to reflect their influence on fire behavior and ignition likelihood.
- Digital elevation model (DEM) [35]: this layer was used to analyze the topography of the study area, considering slope and elevation, which significantly impact fire spread dynamics.

This multi-layered approach allowed for a comprehensive spatial analysis performed by the investigators visually in GIS 3.38, ensuring that ignition points were accurately located in the study area.

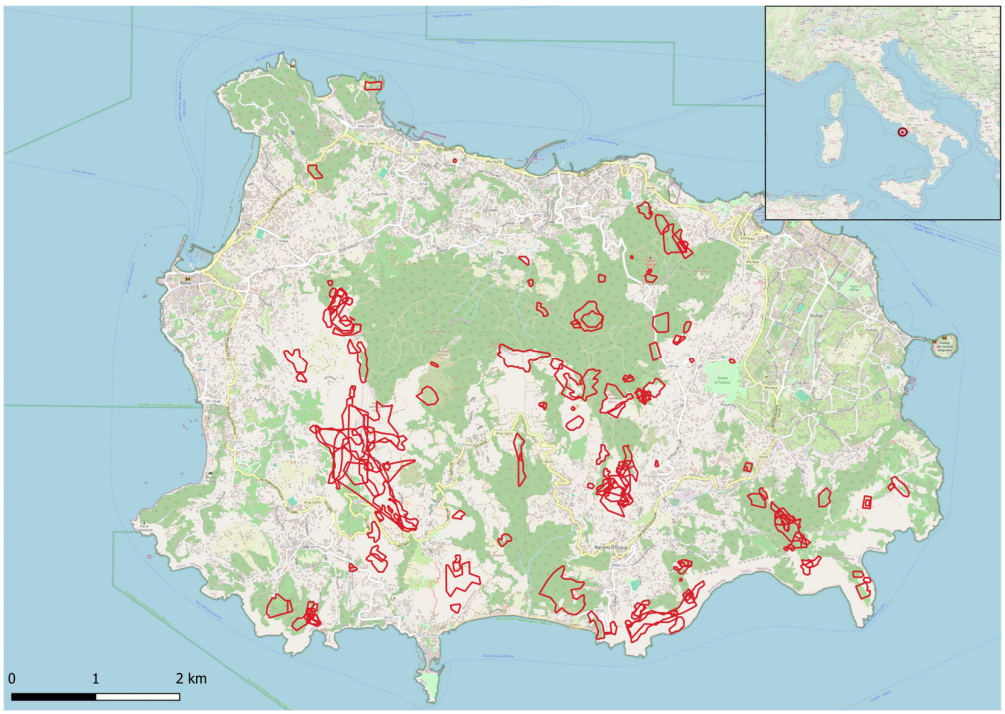

Figure 2. Reconstruction and georeferencing of fire perimeters obtained from the fire register of the Campania region.

Before conducting the subsequent investigations, the habitat map of the Campania region provided by ISPRA [36] and reported in Figure 3, was used to identify the characteristic urban and natural areas of the island.

Based on this territorial classification, the study proceeded to identify the vegetation species distributed across the entire island, which are detailed in Table 1. This classification linked specific vegetation types to their associated fire risks, as different land use types and distributions will also influence ignition likelihood and potential intensity of fires.

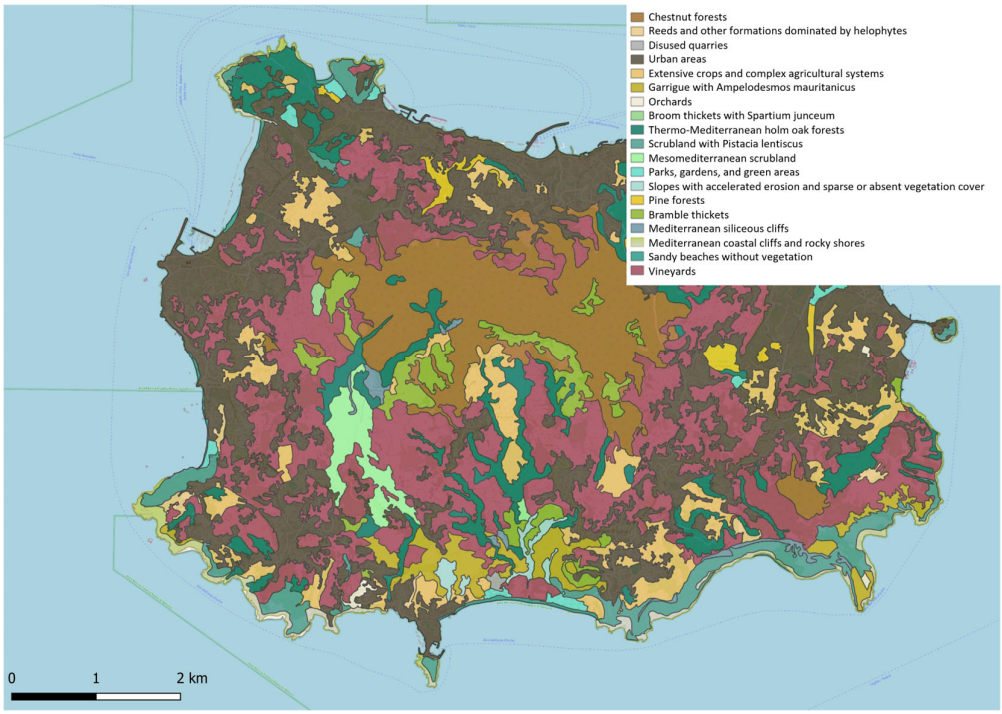

Figure 3. Nature map of the Campania region: habitat map [36].

Table 1. Vegetation types with relative area distribution in Ischia Island.

Vegetation Type	Area (ha)
Bramble	138.56
Mesomediterranean scrub	70.21
Vineyards	1157.92
Thermomediterranean oak forests	400.19
Garrigue	110.79
Chestnut woods	538.68
Pine forests	64.54
Scrub	172.66
Extensive crops and complex agricultural systems	339.41
Broom fields	4.63
Reed beds and other formations dominated by helophytes	22.96
Orchards	6.48

The areas summarized in Table 1 provide an overview of the distribution of vegetation types across the island. This approach is illustrated through the representation of point elements, as highlighted in Figure 4. By linking ignition points to distinct morphological features, this step enhances the accuracy of the fire hazard model, providing a more detailed spatial understanding of ignition likelihood across the study area.

The final step in this phase involved the exclusion of urban areas, as they lack ignition points. Urban areas are likely to experience multiple ignition points, whether intentional or accidental. However, these ignitions are typically short-lived due to the limited availability of combustible materials and the prompt detection and suppression of fires. The vegetation types associated with wildfire ignition on Ischia include bramble, Mediterranean scrub, vineyards, thermos Mediterranean oak forests, garrigue, chestnut woods, pine forest, scrub, and extensive crops and complex agricultural systems.

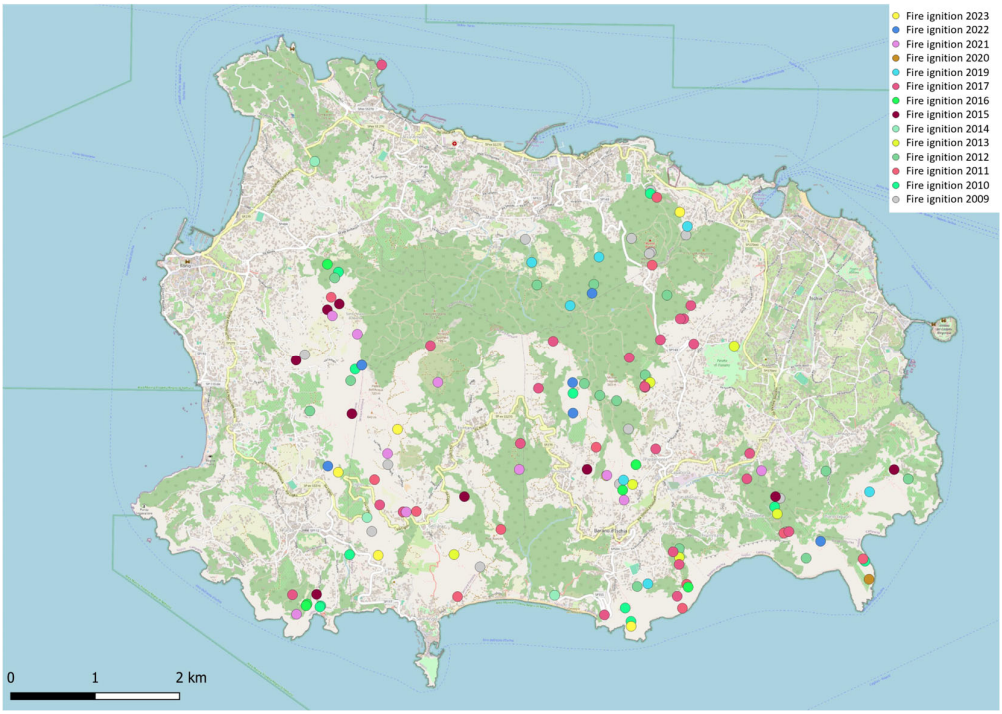

Figure 4. Ignition points related to the fire events that occurred from 2009–2023.

First, the analysis brought out that 75% of the vegetation types present on the island (9 out of 12) have been involved in wildfire ignitions over the last fifteen years. This finding suggests that these vegetation types, in line with land cover patterns, are located in areas more vulnerable to ignition hazards. Additionally, the chemical and physical characteristics of these species can facilitate rapid combustion, highlighting their role in fire risk across the island. As mentioned above, such points are also more vulnerable to sustainment of ignition [37,38].

2.2. Analysis of Wildfire Ignition Causes (2009–2023)

Alongside the reconstruction of fire perimeters on Ischia from 2009 to 2023, an investigation into the potential causes of these fires was essential to identify any recurring factors. Understanding the causes was guided by examining the previously identified ignition points. In this context, two primary factors emerged as significant contributors to fire ignitions:

1. closeness to the road and/or trail network
2. presence of an urban–rural interface zone.

The analysis of ignition point locations in relation to these factors showed that 65% of ignition points were near road or trail networks, while 62% were within urban–rural interface areas. In these zones, the closeness of human infrastructure to natural areas increases the likelihood of ignition, either accidentally or intentionally.

The high density of roads and trails across all sides of the island, as depicted in Figure 5, supports the observation that over half of the fire ignitions may be attributed to human activity. These findings highlight the potential influence of human actions, whether accidental or deliberate, in areas where access to vegetation is facilitated by nearby infrastructure.

The spatial mapping of ignition points, integrated with road and trail network layers, enables the identification of potential correlations between wildfire ignition causes and geographic features. This geospatial visualization contributed to the systematic categorization of urban zones into the vegetation classification β_4 in Table 2 below. The subsequent analy-

sis of potential correlations between ignition points and the influencing factors depicted in Figure 5 provided a robust epistemological basis for excluding β_4-classified areas, justified by the absence of ignition events over an extended temporal horizon.

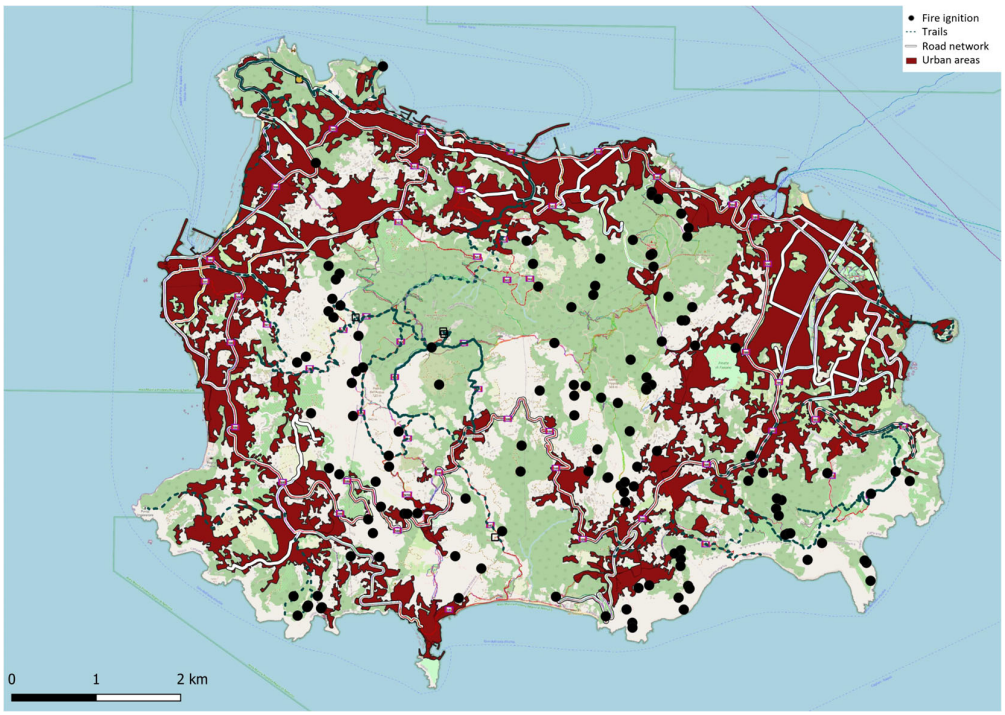

Figure 5. Correlation between ignition points, main road and trail networks, and urban areas on the island.

Table 2. Vegetation types and homogeneous land cover classes.

Homogeneous Land Cover Classes (β)	Vegetation Type	Area (ha)
Permanent crops and vineyards (β_1)	▪ Extensive crops and complex agricultural systems ▪ Vineyards ▪ Orchards	1500.01
Shrublands, thickets, and scrub (β_2)	▪ Scrub with Pistacia lentiscus ▪ Mesomediterranean scrub ▪ Bramble ▪ Garrigue ▪ Reed beds and other formations dominated by helophytes ▪ Broom fields	518.69
Tall vegetation (β_3)	▪ Chestnut woods ▪ Pine forests and Thermomediterranean oak forests	988.08
Urban areas and others (β_4)	▪ Parks, gardens, and green areas	1458.45
Cliffs, slopes, rock formations, quarries, and beaches (β_5)		143.94

2.3. Grouping of Land Cover into Homogeneous Classes

In this study, vegetation types with similar fire behavior potential were grouped into unified classes to streamline analysis. This approach was applied to all remaining

vegetation types that were not associated with a specific characteristic species, ensuring consistent classification across the dataset. The group type classification is summarized in Table 2.

After establishing the new land cover classifications, the resulting map is displayed in Figure 6.

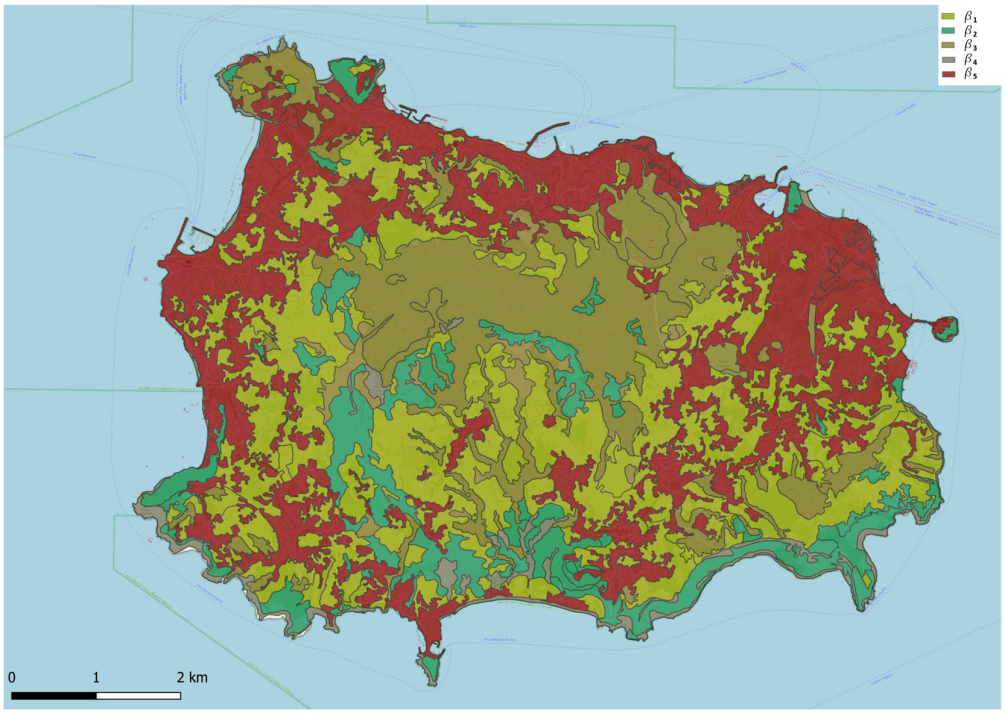

Figure 6. Homogeneous land cover class map.

The process of matching ignition points to homogeneous land cover classes yielded the following percentage distribution. This analysis links each homogeneous land cover class (β_i) with the corresponding number of associated ignition points and calculates the percentage (%) of ignition points for each class. The percentage is determined by dividing the number of fires in each homogeneous class by the total number of recorded fires, providing insights into the relative fire occurrence across different land cover types:

- Permanent crops and vineyards (β_1): 56 ignition points—percentage of 42.42%
- Shrublands, thickets, and scrub (β_2): 46 ignition points—percentage of 34.85%
- Tall vegetation (β_3): 30 ignition points—percentage of 22.73%
- Urban centers and assimilated areas (β_4): 0 ignition points—percentage of 0.00%
- Cliffs, slopes, rock formations, quarries, and beaches (β_5): 0 ignition points—percentage of 0.00%.

The analysis of recorded ignition points confirmed the absence of ignition events within urbanized areas and rocky terrains characterized by minimal or no vegetation cover. Conversely, it highlighted the vegetation cover classes that are more susceptible to fire ignition, as shown in the map in Figure 7.

This map provides a visual representation of regions with heightened susceptibility to wildfire, underscoring the critical need for targeted fire prevention strategies in areas characterized by dense and highly flammable vegetation.

The distribution of ignition points across the homogeneous land cover classes (β_i) demonstrates varying levels of fire susceptibility based on land use. The percentage of ignition points is calculated as the ratio of the number of fires occurring within a specific vegetation class to the total area occupied by that class across the island. This metric

provides a standardized measure of fire incidence relative to vegetation type, enabling meaningful comparisons across different regions or land classifications. Specifically, the percentage of ignition points for each class, calculated as the number of fires in that homogeneous class relative to the total area it occupies, is as follows:

- permanent crops and vineyards ($\beta(_1)$ account for 3.72% of the ignition points.
- shrubs, bushy areas, and maquis (β_2) show a higher percentage at 8.85%.
- high-stem vegetation (β_3) is associated with 2.99% of the ignition points.

Thus, for areas of equal size, the vegetation class most prone to ignition is represented by shrubs, bushy areas, and maquis, followed by permanent crops and vineyards, with high-stem vegetation being the least susceptible. This indicates that certain vegetation types, particularly dense scrublands and maquis, exhibit a higher propensity for ignition due to their structural and compositional characteristics. Conversely, areas with more established, taller vegetation, such as high-stem trees, demonstrate comparatively lower susceptibility to ignition.

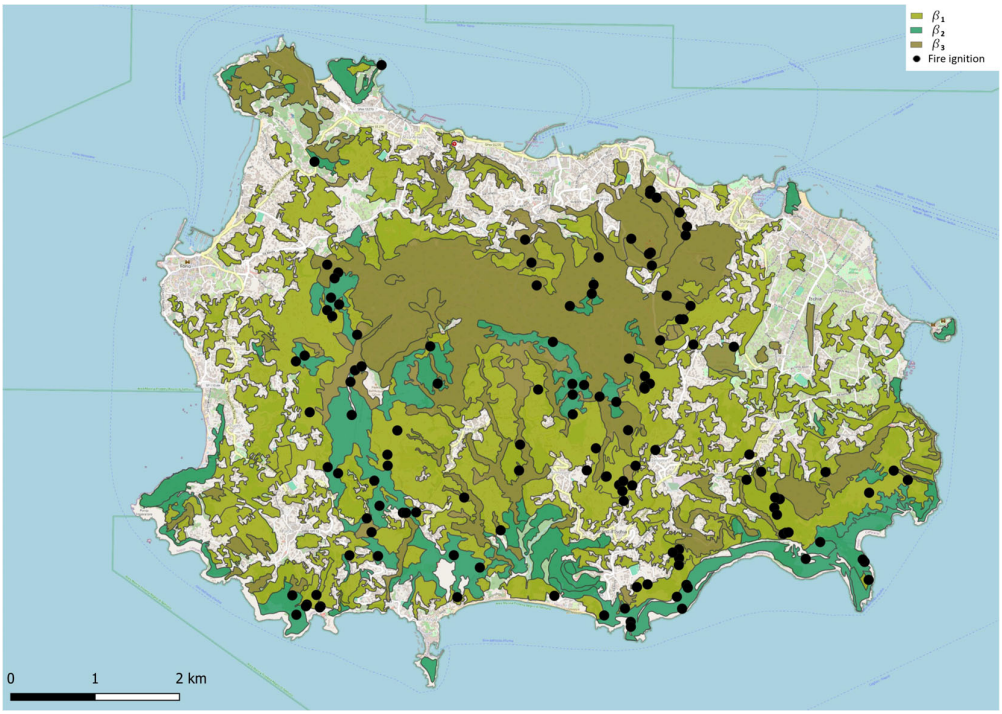

Figure 7. Distribution of ignition points within the homogeneous land cover classes (β_i).

These observations align with the characteristics of the plant species in the class most susceptible to fires, as these species are predominantly distributed throughout the central and southern regions of Ischia. This distribution places them in close proximity to easily accessible roads and natural pathways, which further increases their exposure to ignition. The combination of highly flammable vegetation and the accessibility of these areas contributes to an increased likelihood of ignition in these regions.

The species grouped within the "permanent crops and vineyards" classes are widely distributed across all four slopes of the island, representing the class with the largest area (exceeding 1500 hectares) and consequently highlighting a high rate of involvement in establishing a significant number of ignition points.

High-stem vegetation is primarily concentrated in the central part of the island, particularly around Mount Epomeo (altitude of 787 m a.s.l.). The number of ignition points associated with this vegetation type is lower than in other classes, likely due to its location in higher-altitude, steep, and less accessible areas of the island. This inaccessibility

reduces the likelihood of ignition, as these areas are more isolated from human activity and potential ignition sources. The characteristics of this vegetation type, combined with its challenging terrain, make it less prone to wildfire ignition compared to other, more accessible vegetation classes.

2.4. Poisson Distribution: Spacial–Temporal Analysis and Chi-Square Test

Observations on the location of wildfire ignition points on Ischia from 2009 to 2023 identified three key factors that contribute to forest fire ignition:

- vegetation type at the ignition point;
- closeness to road networks and/or trails, which may facilitate human access and thus potential ignition sources;
- urban–rural interface zones, where the close proximity of human infrastructure and natural areas increases the likelihood of fire ignition.

Given these factors, we now evaluate the probability that, within a defined area and time frame, one or more ignition events may occur in the future, as depicted in Figure 8. Such an assessment is crucial because, while wildfires are frequently linked to human activities and can be unpredictable, they display a continuity within specific homogeneous areas that are more prone to ignition.

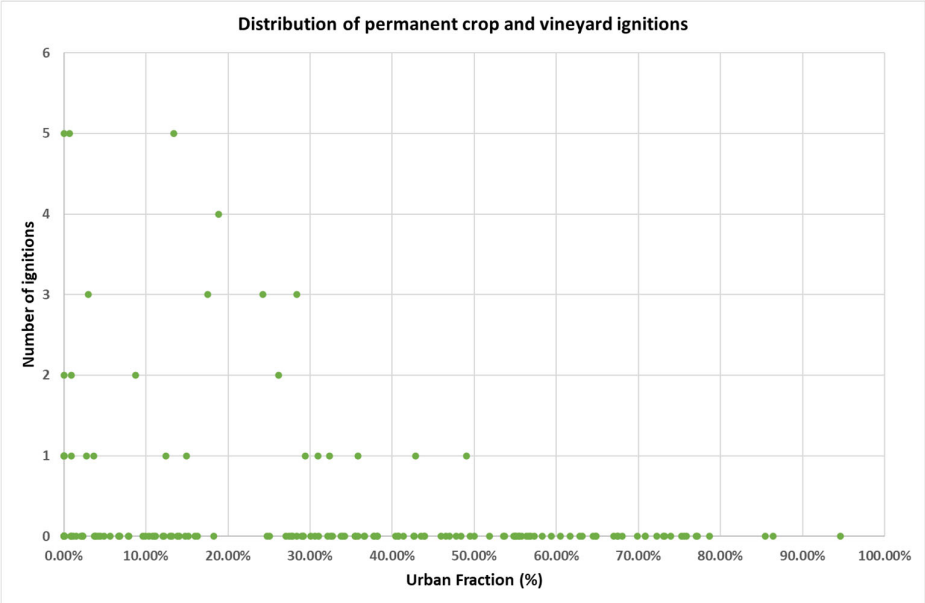

Figure 8. Distribution of ignitions related to the homogeneous land cover class "permanent crops and vineyards" as a function of the percentage of the urban fraction in the occupied cell.

The island is divided into cell sizes 500 m by 500 m, as shown in Figure 9. From a total number of 336 cells, only 212 (63% of the total number) refer to land and exclusively contain the plant species associated with the previously examined land cover classes, namely β_1, β_2, and β_3.

We model the spatial–temporal distribution of ignition points using a Poisson process, whose non-stationary geographic intensity is described by the function $\lambda(x)$, defined in a geographic domain R^2 where x represents a couple of coordinates of a generic point of interest within the domain itself.

The application of the probabilistic Poisson model implies that ignition points are "statistically independent" and locally "equiprobable." From statistical independence, it follows that the events previously recorded during the observation period do not influence the spatial and temporal localization of future ignitions [39].

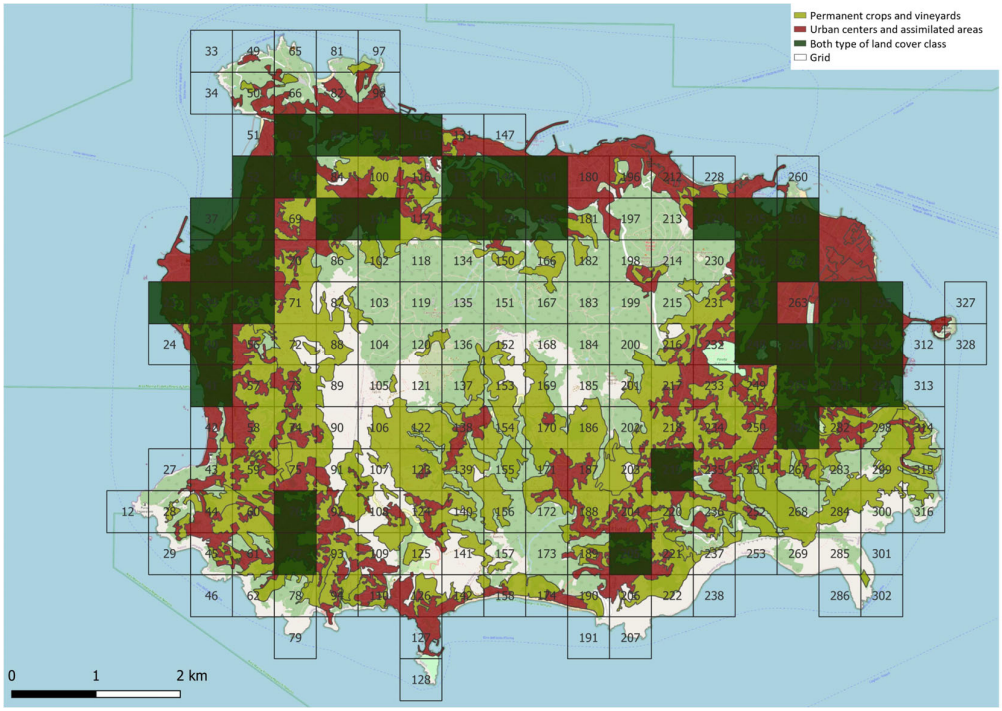

Figure 9. Grid cells in dark green simultaneously occupied by the homogeneous land cover class "permanent crops and vineyards" and the homogeneous land cover class "urban centers and assimilated areas" with a percentage greater than 50%.

For a given area, the probability that the number K of ignition points in the area equals n within the time interval [0, t] is represented by the discrete Poisson distribution as shown in Equation (1).

$$P(K = n) = \frac{(\lambda \Delta t)^n}{n!} e^{-\lambda \Delta t} \quad (1)$$

Equation (1). Poisson Distribution Law.

where:

- $n \in \mathrm{N}$ represents the number of ignition points considered;
- λ represents the Poisson Hazard Rate, i.e., the average rate of events related to a specific area and a given time horizon

$(\Delta t = 1,\ \mathrm{where}\Delta \mathrm{tisthelenghtoftimeintervalconsidered})$;

- $\frac{1}{\lambda}$ represents the average waiting time expressed in years for an event, commonly referred to as the return period.

In order for the Poisson process with intensity $\lambda > 0$, the following conditions hold:

- $K(0) = 0$: counting of events starts from the initial moment;
- $K(t)$ has independent increments;
- the number of events in any interval of length $t > 0$ has Poisson (λt) distribution (stationarity of increments);
- $\frac{P[K(h)=1]}{h} = \lambda$: in a very small time interval [0, h], the probability of a single event approaches λh in the limit;
- $\frac{P[K(h)>2]}{h} = 0$: in a small time interval [0, h], the probability of more than one single event approaches zero faster than h in the limit.

Considering only the time variable, it is as if all the ignition events recorded from 2009 to 2023 lose their regional classification and occur in a homogeneous land cover, being classified based on the year of occurrence. Now consider three areas, each covering land

cover classes: $\boldsymbol{\beta_1}$, permanent crops and vineyards $\boldsymbol{\beta_2}$, shrublands, bushes, and scrublands, $\boldsymbol{\beta_3}$, tall vegetation, three different specific rate $\boldsymbol{\lambda}'$ are calculated, respectively $\boldsymbol{\lambda}'_{\boldsymbol{\beta 1}}$, $\boldsymbol{\lambda}'_{\boldsymbol{\beta 2}}$ and $\boldsymbol{\lambda}'_{\boldsymbol{\beta 3}}$, by dividing the ignition points of each homogeneous class and years.

$$\boldsymbol{\lambda}'_{\boldsymbol{\beta i}} = \frac{\boldsymbol{n}(\boldsymbol{\beta_i})}{\boldsymbol{num.years.obs.}} \quad (2)$$

Equation (2). Average specific rate of events occurring over the annual time period within the homogeneous land cover class β_i
where:

- $\boldsymbol{\lambda}'_{\boldsymbol{\beta i}}$: average specific rate of ignition points occurred in $\boldsymbol{\beta}_i$;
- $\boldsymbol{n}(\boldsymbol{\beta}_i)$: number of times ignition points which occur in $\boldsymbol{\beta}_i$;
- ***num.years.obs.***: number of years within the observation period during which ignition events were recorded across the homogeneous land cover class $\boldsymbol{\beta}_i$.

The spatial distribution of ignition points is integrated into the numerical model to estimate the annual probability of one or more fires occurring within a single grid cell B_j. The analysis of available datasets, combined with the integration of the land cover vector layer on the grid, revealed that ignition points are predominantly concentrated in areas classified as permanent crops and vineyards, shrublands, bushes, scrublands, and tall vegetation, collectively categorized under homogeneous land cover class as β_i (i = 1,..,3).

The rate $\lambda'_{\beta i}$ of the Poisson process associated with a single cell B_j $\lambda_{\beta_i}(B_j)$ is to be proportional to the areal extent $A_{\beta_i}(B_j)$ of the three specified land cover types within the *j*-th cell). Accordingly, the computation of the parameters $\lambda_{\beta_i}(B_j)$ is governed by the following equation.

$$\lambda_{\beta i}(B_j) = \frac{m_{\beta i}(B_j)}{num.\ years.\ obs.} x\ A_{\beta_i}(B_j) \quad (3)$$

Equation (3). Average rate of occurrence $\lambda_{\beta i Ai}(B_j)$ in a *j-th* cell.

The value of $\lambda_{\beta i}(B_j)$ *is* equal to the average number of ignition points for the homogeneous land cover class β $\left(E\left|n_{\beta i}(B_j)\right|\right)$.

The representation that approximates the value of the proportionality coefficient $m_{\beta i}$ is described in the following Equation (4).

$$m_{\beta i} = \frac{\sum n_{iK}(B_j)}{A_{\beta_i}(B_j)} \quad (4)$$

Equation (4). Proportionality coefficient refers to each homogeneous land cover class β_i.

Here,

- $\sum n_{iK}(B_j)$: represents the sum of ignition points K for the homogeneous land cover class β_i in the *j-th* cell;
- $A_{\beta_i}(B_j)$: represents the area occupied by the homogeneous land cover class β_i within the *j-th* cell, that is, the total area of the considered homogeneous land cover class.

The estimation of parameters $\lambda_{\beta i}(B_j)$ for each cell allows calculation of the probability of one or more ignition events occurring within the land cover class of each cell.

$$P(K) = \frac{\left[\lambda_{\beta i Ai}(B_j)\ \right]^k}{k!} e^{-\lambda_{\beta i Ai}(B_j)} \quad (5)$$

Equation (5). Discrete Poisson probability distribution related to the cell B_j.

After estimating the Poisson hazard rate (λ) for each cell combined rates of each homogeneous land cover class, it is essential to verify whether the rate derived from

historical observations accurately represents the studied phenomenon. Additionally, it is advisable to assess the consistency of the ignition event data with the Poisson distribution. The validity of the chosen probability distribution model for representing the randomness of wildfire ignition can be statistically confirmed or refuted using the chi-square test.

The chi-square test was used to verify whether the observed frequency values (ignition events) align with the theoretical frequencies of the Poisson distribution [40]. The chi-square test operates under several key assumptions: independence of observations, sufficiently large expected frequencies, categorical data, comparison against a theoretical distribution, and adequately large sample size to ensure statistical reliability. While expected cell frequencies below five may not substantially impact the Type I error rate, they can significantly reduce the statistical power of the test. This underscores the necessity of employing large sample sizes to enhance the robustness and reliability of the results, particularly in cases involving small expected values [41].

To perform the chi-squared test, a sample consisting of n observations of a specific variable is partitioned into K distinct categories. For each category, the expected frequency is calculated, representing the frequency that would be observed under the assumption that the sample data follow the hypothesized distribution. The test involves assessing the concordance between the experimental distribution and the theoretical distribution by comparing the observed frequencies with the expected frequencies calculated using the lambda values for each land cover class according to the Poisson distribution. A greater deviation between the observed and expected values suggests a stronger deviation from the hypothesized distribution, which may indicate a significant relationship between the two variables under investigation.

If the observed frequencies align exactly with the expected frequencies, it can be inferred that the two variables are perfectly independent. To ensure the validity of the chi-squared test, it is essential that the expected frequencies meet a minimum threshold of five; otherwise, the test may produce unreliable results, potentially leading to substantial deviations from the expected distribution.

Application to the Case Study

By correlating the information obtained from the spatial–temporal analysis with the homogeneous land cover classes examined (β_i), it was possible to derive the associated Poisson lambda. In this regard, the estimation was first carried out with reference to the occupation of the three homogeneous cover classes representative of the study in question:

- $\lambda_{\beta 1 A1}$: for the homogeneous land cover class designated as "permanent crops and vineyards" encompassing a total area of 1500.01 ha
- $\lambda_{\beta 2 A2}$: for the homogeneous land cover class designated as "Shrublands, bushes, and scrublands" encompassing a total area of 518.69 ha
- $\lambda_{\beta 3 A3}$: for the homogeneous land cover class designated as "Tall vegetation" encompassing a total area of 988.08 ha.

Afterward, the ignitions that occurred in the last fifteen years (2009–2023) were recorded and categorized according to each of the three examined classes:

- "permanent crops and vineyards" $n_{1k}(\beta 1)$: 56
- "*Shrublands, bushes, and scrublands*" $n_{2k}(\beta 2)$: 46
- "*Tall vegetation*" $n_{3k}(\beta 3)$: 30.

Using the spatial distribution maps of land cover classes and ignition events generated in QGIS, a preliminary quantitative analysis was conducted on the two least impacted land cover classes, specifically "permanent crops and vineyards" and "tall vegetation", This analysis was performed prior to the calculation of the Poisson rate λ and aimed to

investigate the absence of ignition events within the specific cells associated with these classes over the past fifteen years.

For the land cover class corresponding to "permanent crops and vineyards", which is extensively distributed across the island's territory, particularly near inhabited areas, the potential inclusion of urbanized fractions within individual cells was systematically analyzed.

The results were presented in the scatter diagram shown in Figure 8, which highlights the observed trends.

This analysis aimed to confirm whether cells with a relatively high proportion of urbanized areas exhibited low or nearly zero ignition occurrences during the observation period, as anticipated. In areas characterized by high urban density, the probability of wildfire ignition in small vegetation patches is significantly reduced, primarily due to the limited time available for arsonists to start a fire. Furthermore, documenting human-initiated ignition is very challenging, especially in urban areas where such incidents are often rapidly suppressed. The results depicted in the scatter diagram (Figure 8) confirmed this hypothesis, showing no recorded ignition points in cells where the proportion of urban areas exceeded a 50% threshold. However, to ensure a statistically robust and representative estimation of the Poisson rate λ for the homogeneous land cover class "permanent crops and vineyards," all cells within this class were included in the analysis. While the high urban fraction in these cells suggests a reduced probability of arson, Figure 9 demonstrates that the hypothesis of potential ignition from natural causes (such as spontaneous combustion or lightning) or accidental causes still holds true.

For the class corresponding to tall vegetation, cells with an occupancy rate exceeding 75% were predominantly located at higher elevations on the island. A geographical analysis was performed to verify whether the absence of ignition events within these cells correlated with altitude.

Specifically, the maximum elevation of each cell within this class was recorded and analyzed in relation to the topographical features of the corresponding area, as illustrated in Figure 10.

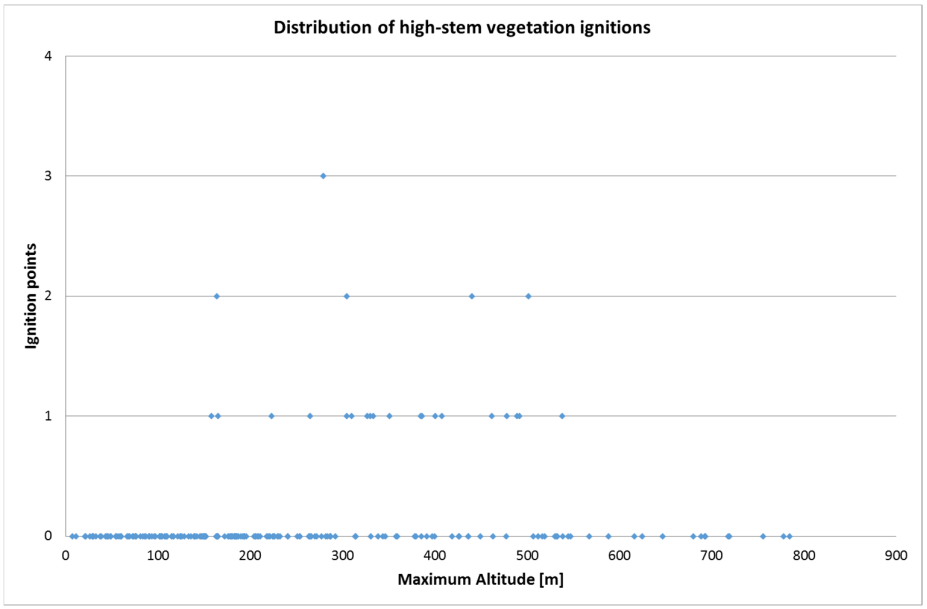

Figure 10. Distribution of ignitions related to the homogeneous land cover class "tall vegetation" as a function of the maximum elevation of the corresponding cell.

An analysis of the scatter diagram illustrating the distribution of ignition events in tall vegetation as a function of the maximum elevation for all occupied cells (Figure 10)

revealed that ignitions within this class occur exclusively below an elevation threshold of approximately 550 m. Consequently, in Figure 11, following the same methodology used for permanent crops, all grid cells within this class were included in the calculation of the Poisson rate λ, even those located at elevations greater than or equal to 550 m, to ensure a representative estimation of the fire hazard associated with this land cover class.

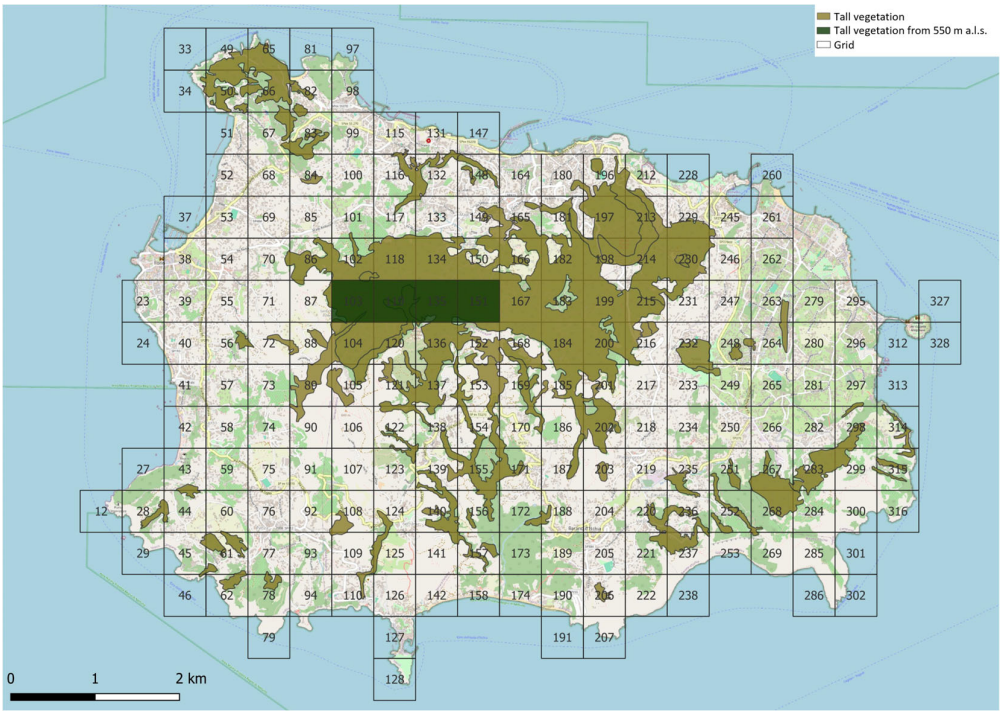

Figure 11. Grid cells, in dark green, occupied by the homogeneous land cover class "tall vegetation" with an elevation greater than 550 m a.l.s.

These cells represent a portion of the island's territory that is particularly difficult to access, and therefore, more challenging to ignite. This accessibility issue explains why no ignitions have been recorded in these areas during the past fifteen years of observation.

With regard to the location of the 132 fires recorded during the observation period, the average ignition event rate for each individual cell B_j, based on the spatial distribution of the respective land cover class within the cell, was calculated as follows:

$$E\left|n_{\beta i}(B_j)\right| = \lambda_{\beta i A i}(B_j) = \frac{m_{\beta i}}{num.\,years.\,obs.}\; x\; A_{\beta i}(B_j) \tag{6}$$

Equation (6). Discrete Poisson probability distribution related to the cell B_j.

Where the following values are obtained according to Equation (4):

- $m_{\beta 1} = 0.0373$
- $m_{\beta 2} = 0.0887$
- $m_{\beta 3} = 0.0304$

The average ignition event rate for each class β_i, referring exclusively to the time variable "years of observation," was instead calculated as stated in the previous Poisson hazard rate equation.

- $\lambda_{\beta 1} = 3.7333$
- $\lambda_{\beta 2} = 3.0667$
- $\lambda_{\beta 3} = 2.0000$

Once the lambda values associated with the individual grid cells and the homogeneous land cover classes, based on the observation period, were obtained, the subsequent step was to determine the parameters required for applying the chi-square test, in both spatial and temporal analysis.

Furthermore, two separate tests were applied to evaluate the accuracy of the expected results:

1. spatial validation of parameter $\lambda_{\beta S}$;
2. temporal validation of parameter $\lambda_{\beta T}$.

The application of the chi-square test was carried out with reference to an explanatory table containing the representative data for each examined homogeneous land cover class (β_i).

For the spatial validation of the chi-square test the following graphical representations in Figure 12a–c show the observed frequencies of fires within the homogeneous land cover classes and the corresponding probability.

After computing the frequencies for the three distinct homogeneous land cover classes, the subsequent step involved validating the statistical representativeness of the Poisson rate lambda (λ). This involved comparing the observed fire frequencies with the expected frequencies derived from the Poisson distribution model, thereby verifying the robustness and precision of the lambda estimates for each class. According to the spatio-temporal analysis performed, which facilitated the estimation of the spatial and temporal rates of the Poisson distribution, the chi-square test was applied to both the classes defined by the spatial parameter as in Table 3 (vegetation cover type) and those categorized by the temporal parameter (individual year of observation).

Table 3. Spatial validation test results.

Homogeneous Land Cover Classes (β_i)	$\lambda_{\beta S}$	Degree of Freedom	Threshold Value	χ^2 Value	Test Result
Permanent crops and vineyards (β_1)	0.0200	4	9.488	3.4930	positive
Shrublands, thickets, and scrub (β_2)	0.0258	3	7.815	5.3774	positive
Tall vegetation (β_3)	0.0154	2	5.991	0.7861	positive

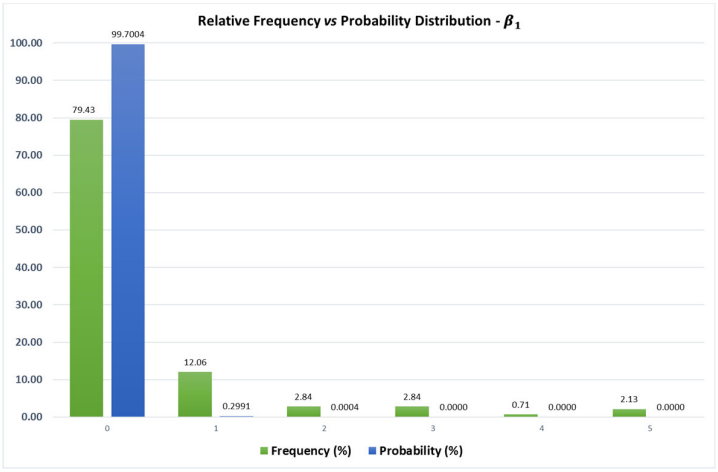

(**a**)

Figure 12. *Cont.*

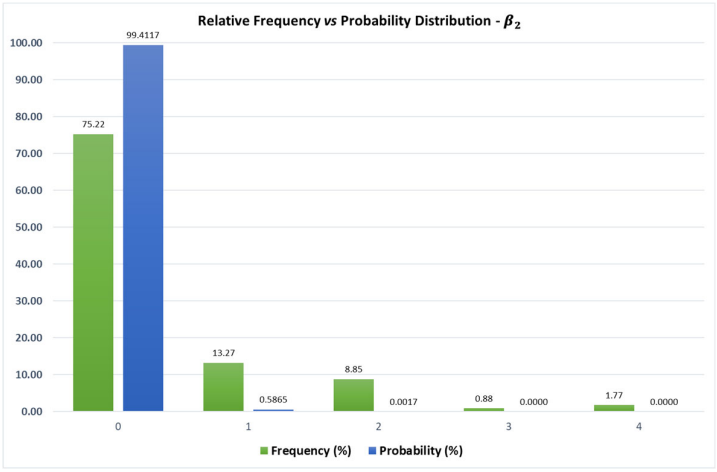

(**b**)

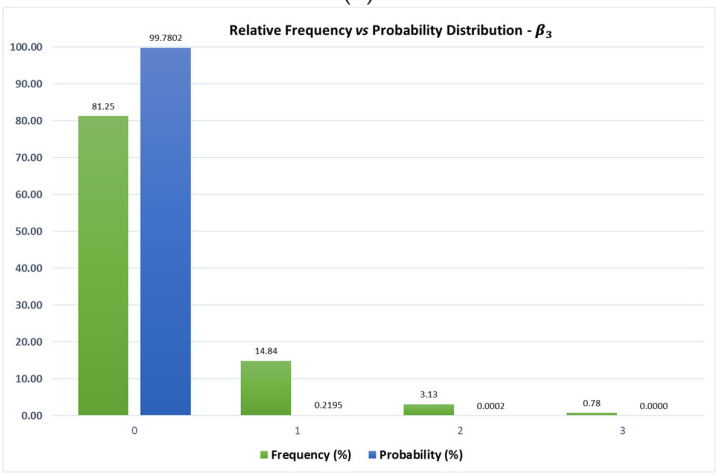

(**c**)

Figure 12. Spatial analysis: (**a**) relative frequency and probability distribution for β_1 ; (**b**) relative frequency and probability distribution for β_2; (**c**) relative frequency and probability distribution for β_3.

For the temporal validation of the dataset, the chi-square test was applied by first partitioning the recorded fire occurrences over the observed period (2009–2023) within each homogeneous land cover class, as illustrated in Table 4.

Table 4. Number of fires over the observed period in the homogeneous land cover classes.

	2009	2010	2011	2012	2013	2014	2015	2016	2017	2018	2019	2020	2021	2022	2023
β_1	3	4	4	6	5	1	6	2	15	/	3	/	6	/	1
β_2	3	6	6	5	1	1	2	3	6	/	/	1	4	5	3
β_3	8	1	3	5	1	1	1	1	3	/	4	/	/	1	1

For the temporal validation of the chi-square test the following graphical representations in Figure 13a–c show the frequencies of fires calculated in the homogeneous land cover classes and the probability comparisons.

Following the calculation of frequencies for the three distinct homogeneous land cover classes, the subsequent step involved validating the statistical representativeness of the Poisson rate lambda (λ) as showed in Table 5. This was achieved through the application of the previously described Table 4, which facilitated the comparison of observed fire

frequencies with the expected frequencies derived from the Poisson distribution model, thereby ensuring the reliability and precision of the lambda values for each class.

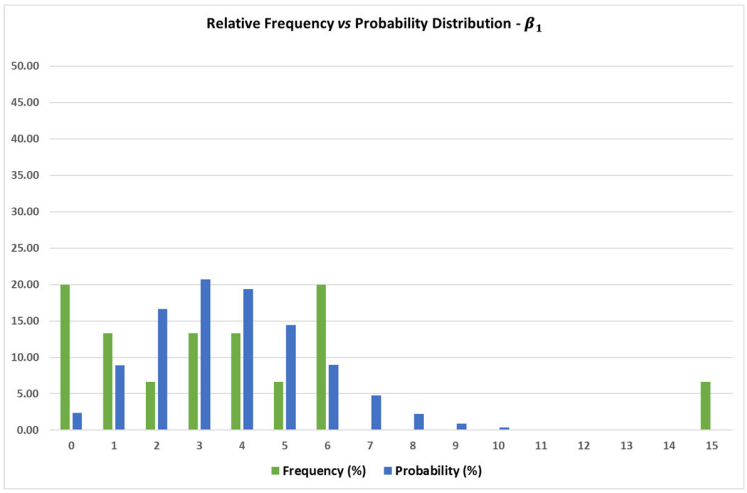

(**a**)

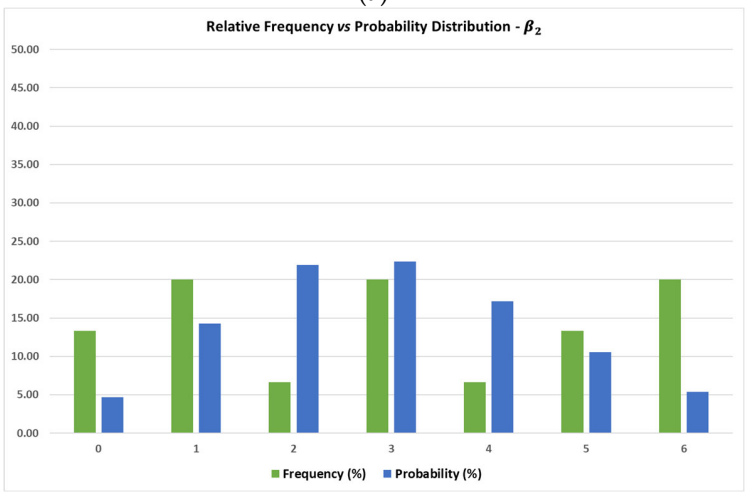

(**b**)

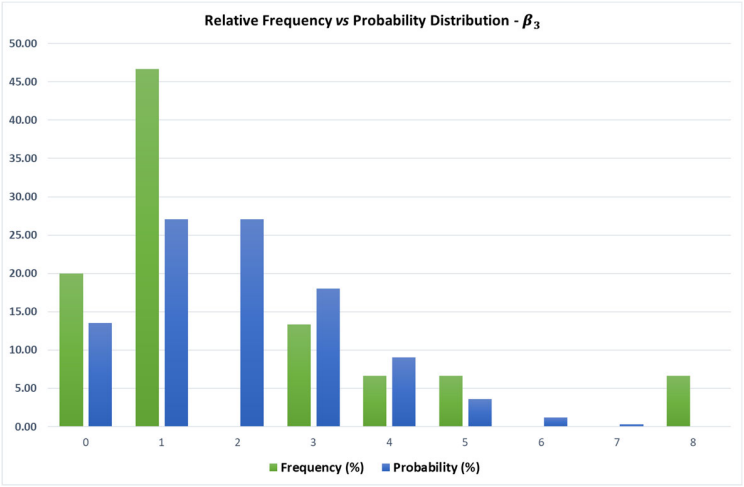

(**c**)

Figure 13. Temporal analysis: (**a**) relative frequency and probability distribution for β_1 ; (**b**) relative frequency and probability distribution for β_2; (**c**) relative frequency and probability distribution for β_3.

Table 5. Temporal validation test results.

Homogeneous Land Cover Classes (β_i)	$\lambda_{\beta T}$	Degree of Freedom	Threshold Value	χ^2 Value	Test Result
Permanent crops and vineyards (β_1)	3.7333	6	12.592	1.903	positive
Shrublands, thickets, and scrub (β_2)	3.0667	5	11.071	3.046	positive
Tall vegetation (β_3)	2.0000	4	9.488	6.929	positive

The equations presented in Section 2 are now applied to estimating the local wildfire ignition hazard on the island of Ischia based on the homogeneous land cover classes analyzed in Section 3.

3. Results

In this section, the results are discussed in accordance with the procedure outlined in Section 2.

After completing the validation of the statistical representativeness of the parameters $\lambda_{\beta iAi}$, (for spatial validation) and $\lambda_{\beta i}$, (for temporal validation), the analysis focused on calculating the probability that the number of ignition events $K = 0$ occurs within a year for each grid cell associated with a specific land cover class.

$$K = 0 \rightarrow P_{\beta i}\left[n_{ik}(B_j) = 0\right] = \frac{\lambda_{\beta iAi}(B_j)^0}{0!} e^{-\lambda_{\beta iAi}(B_j)}$$

Using the Poisson probability distribution, the probability for n_K = 0 over a one-year time horizon was calculated for the *j-th* cell, which is occupied by the homogeneous land cover class.

Subsequently, the probability of observing a number of ignition events $K \geq 1$ was determined as the complement of the probability for $K = 0$:

$$K \geq 1 \rightarrow P_{\beta i}\left[n_{iK}(B_j) \geq 1\right] = 1 - P\left[n_{\beta i}(B_j) = 0\right]$$

The Poisson probability distribution $n_K \geq 1$ over a one-year time horizon was calculated for the *j-th* cell, which is occupied by the homogeneous land cover class B_j.

The corresponding return period for each cell was calculated as follows:

$$T_r[years] = \frac{1}{P\left[n_{ik}(B_J) \geq 1\right]} \quad (7)$$

Equation (7). Return period for $P\left[n_{ik}(B_J) \geq 1\right]$.

Upon completing the acquisition of the local hazard levels and the corresponding return times for the *j-th* cells within each land cover class, the next step involved calculating the ignition probabilities for the individual homogeneous land cover classes β_i.

$$P_{\beta_i}(n_{iK} \geq 1) = 1 - P_{\beta_i}\left(n_{ik}(B_j) = 0\right) \quad (8)$$

Equation (8). Probability estimation $P\left[n_{ik}(B_J) \geq 1\right]$.

Given the probabilities of observing one or more ignition events within a year for each land cover class, the corresponding return time was calculated using Equation (7).

Next, based on the ignition probabilities of the individual land cover classes present within each grid cell, the corresponding return times were then calculated. For each cell, the overall probability of observing one or more ignition events $\left(P_{\beta i}\left[n_{iK}(B_j) \geq 1\right]\right)$ within

the annual time frame was calculated by summing the probabilities of all homogeneous land cover classes present in that cell:

$$P_{\beta i}\left[n_{iK}\left(B_j\right) \geq 1\right] = \sum_{i=1}^{3}\left[1 - P_{\beta_i}\left(n_{iK}\left(B_j\right) = 0\right)\right] \quad (9)$$

Equation (9). Probability for $n_{ik} \geq 1$ obtained by summing the probabilities recorded for each homogeneous land cover class present within the *j—th* cell.

Where n_{iK} represents the number of land cover classes contained within the individual cell. The study was divided into two specific analyses, considering the categorization of grid cells based on their land cover class.

The first analysis focused on land cover classes β_4 ("urban centers and assimilated areas") and β_5 ("cliffs, slopes, shorelines, quarries, and beaches"). For these classes, an ignition probability close to zero was assumed based on the data recorded in the Wildfire Registry of the Campania Region. This assumption is supported by the fact that no ignition events were documented in these areas during the observation period from 2009 to 2023: $P_{\beta_4,\,\beta_5}(s,t) \sim 0$.

The absence of ignition events in these classes is attributed to minimal vegetation cover and reduced fuel availability, alongside geographical or infrastructural conditions that further decrease the likelihood of ignition.

The second analysis examined the classes β_1, β_2 and β_3, considering the special conditions for β_1 and β_3, influenced, respectively, by the presence of urban areas and the elevation of the terrain.

In this context, the probabilities and their respective return times were calculated as follows in Table 6.

Table 6. Probabilities and return times for homogeneous land cover classes β_i.

Homogeneous Land Cover Classes (β_i)	$P_{\beta_i}(n_{ik}=0)$	$P_{\beta_i}(n_{iK}\geq 1)$	T_r[Years]
Permanent crops and vineyards (β_1)	0.0240	0.9760	1.02
Shrublands, thickets, and scrub (β_2)	0.0466	0.9534	1.05
Tall vegetation (β_3)	0.1354	0.8646	1.16

These probability values in column $P_{\beta_1}(n_{ik} = 0)$ represent the probability of recording zero ignition events in a year for the respective land cover classes β_i. Consequently, the complementary probability was calculated to determine the likelihood of observing one or more ignition events $K \geq 1$ within the same timeframe. Moreover, the return time yielded the following results is depicted. By analyzing the data derived from the calculations described above, a map was generated to illustrate the distribution of probabilities associated with the *j-th* grid cells.

Specifically, the ignition probability for each examined grid cell was distributed as shown in Figure 14.

Analyzing the results obtained, it emerged that in an area covered by the examined land cover classes β_1, β_2 and β_3, totaling approximately 5300 hectares and appropriately divided into 212 cells, about 60% shows a probability between 0.0100 and 0.0200 of recording one or more ignitions (K > 1) within the annual time frame, while around 40% shows a probability close to 0 in the same time period. As expected, most of the cells associated with the highest ignition probabilities are characterized by the co-presence of the three examined land cover classes and, at the same time, are adjacent to the main road and trail networks of the island, where arson activities are more frequent and predictable. Furthermore, these areas are characterized by the presence of fuels capable of ensuring rapid fire spread (shrublands, vineyards, scrublands, chestnut trees, and oaks), but above

all, by the absence of interruptions to the continuity of these fuels, which could otherwise create gaps that might slow down or even stop the fire.

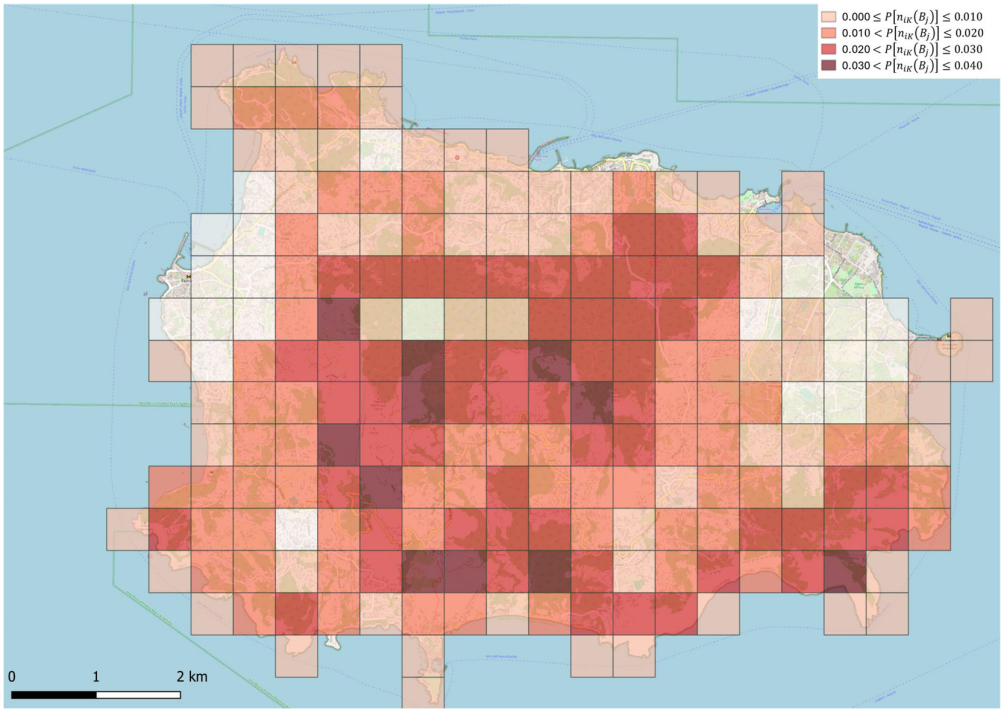

Figure 14. Hazard map of probability ignition points in Ischia Island.

4. Discussion

The study outlined in Section 2 aims to analyze the spatial–temporal patterns of wildfire occurrences on the island of Ischia, with the ultimate goal of developing strategies for wildfire risk mitigation. The study is organized into several phases, outlined in Figure 1, including data collection, land cover classification, and the application of statistical models, such as the Poisson distribution and chi-square test, used to validate the sample data in order to obtain robust hazard maps.

By categorizing the island's land cover into homogeneous classes (e.g., permanent crops and vineyards, shrublands, and tall vegetation), the study simplifies the analysis while improving the accuracy of hazard estimations. This classification highlights the varying susceptibility to fire risk, with certain vegetation types more prone to ignition due to their physical and chemical properties. By combining these thematic layers, the analysis achieved a more reliable foundation for subsequent wildfire risk assessment and mapping, allowing for precise evaluations aligned with the physical and environmental characteristics of the region. For instance, scrublands and shrub thickets were found to be the most vulnerable, representing 8.85% of the ignition points, followed by vineyards and permanent crops at 3.72%. These findings underscore the importance of vegetation management in wildfire prevention, suggesting that more frequent interventions (e.g., clearing, controlled burns) could be beneficial in high-risk areas. By systematically categorizing these vegetation types, the study laid the foundation for more accurate hazard estimation across various land cover classes, contributing to a targeted approach in wildfire risk assessment.

The study detailed in Section 2 focuses on analyzing the spatiotemporal patterns of wildfire occurrences on the island of Ischia, aiming to support the development of effective wildfire risk mitigation strategies. The methodology was structured as a multi-phase process to systematically address the research objectives and ensure comprehensive analysis.

Initially, historical wildfire event data from 2009 to 2023 were collected and analyzed to identify ignition points and their spatial distribution. The ignition points were georeferenced through satellite imagery and field data, then integrated with thematic geospatial layers, encompassing vegetation types, land use patterns, and proximity to urbanized areas. This integration facilitated a detailed stratification of the land cover into homogeneous categories—such as permanent crops and vineyards, shrublands, and tall vegetation—which formed the analytical basis for the wildfire assessment.

In Section 3, a probabilistic modeling approach was adopted, using the Poisson distribution to estimate wildfire ignition probabilities across specific land cover classes over time. The model was validated through chi-square tests, ensuring statistical robustness of the results. The analysis incorporated critical factors such as vegetation type, road proximity, and elevation, providing nuanced insights into wildfire risk dynamics.

The results highlighted the susceptibility of different land cover classes: shrublands and thickets were identified as the most vulnerable, accounting for 8.85% of ignition points, followed by permanent crops and vineyards at 3.72%. These findings emphasize the necessity of integrating physical and environmental variables into wildfire hazard assessments to enhance predictive accuracy.

The analysis of the results revealed that for cells associated with the land cover classes β_1, β_2 and β_3, the probability of a wildfire ignition in the upcoming year is always greater than zero.

To validate the dataset and its distribution, a chi-square test was applied. This provided both spatial and temporal validation, which is essential to account for the unique characteristics of wildfires, particularly their dependence on land use and seasonal trends [42].

Finally, the estimation of local and global wildfire hazards across homogeneous land cover classes provides valuable insights for policymakers and land managers. On a local scale, identifying high-risk areas, as shown in red in Figure 14 enables more effective and targeted interventions, such as the strategic allocation of firefighting resources and improved land use planning.

5. Conclusions

This study contributes to understanding wildfire risk on the island of Ischia by providing a detailed spatial–temporal analysis of ignition points and hazard estimations for various land cover types. The use of Poisson distribution modeling, validated through a chi-square test, establishes a robust framework for assessing wildfire risks in Mediterranean regions. The findings offer a foundation for developing targeted mitigation strategies in future research.

Despite the study's approximations, primarily due to the limited availability of input data for calculating ignition probabilities, the resulting hazard map effectively identifies areas most predisposed to wildfires. High probabilities of ignition, combined with intensity and vulnerability factors, significantly impact the resilience of the site and are likely to continue doing so.

The creation of regionalized hazard maps emerges as a crucial resource for forecasting and prevention activities, as well as for the efficient allocation of resources in the management and planning of the territory. By analyzing factors that predispose specific areas to fire, this study enables the proactive identification of regions requiring targeted interventions for risk reduction and mitigation efforts.

Specifically, the findings of this study could inform future land-use planning, improve surveillance, and enhance monitoring activities, particularly in areas of high natural and landscape value. In these regions, wildfires tend to have a more substantial ecological and

social impact and are more challenging to manage due to the topography, as illustrated by the historical fire data from 2009 to 2023.

These considerations underscore the need for additional security and surveillance measures, such as installing thermal cameras along paths near roads and urban areas. Such measures would help counteract harmful activities and reduce the likelihood of wildfire ignition. Additionally, it is essential to develop a constantly updated plan for efficient firefighting operations by civil protection teams, ensuring rapid responses in the island's most vulnerable and challenging areas.

The model's robustness could be improved by incorporating proximity criteria for roads and trails. Integrating the distance between ignition points and access routes would facilitate the analysis of correlations between arson events and the accessibility or usability of pathways leading to ignition sites. This addition would offer a more nuanced understanding of the spatial dynamics influencing wildfire occurrences.

Another critical aspect is the potential domino effect of wildfires. Post-event landslide susceptibility maps should be analyzed to assess whether wildfire-induced soil degradation, in combination with heavy rainfall, serves as a precursor to landslide mobilization. This investigation would yield essential insights for mitigating secondary hazards associated with wildfires and enhancing comprehensive risk management strategies. The analysis also highlights the critical importance of urban–rural interface zones, where increased human activity renders existing vegetation more susceptible to fires. In these zones, preventive planning is essential to avoid catastrophic consequences, not only for infrastructure but also for the local population. Therefore, drafting up-to-date evacuation plans aligned with the identified hazards is vital for ensuring the safety of residents in the event of a wildfire.

Author Contributions: Conceptualization, D.B., M.G., A.L. and M.L.; methodology, D.B., M.G., A.L. and M.L.; validation, D.B. and M.L.; writing, review and editing, D.B., M.G. and M.L. All authors have read and agreed to the published version of the manuscript.

Funding: This research received no external funding.

Data Availability Statement: The raw data supporting the conclusions of this article will be made available by the authors on request.

Acknowledgments: This study was carried out within the RETURN Extended Partnership from the European Union Next-GenerationEU (National Recovery and Resilience Plan—NRRP, Mission 4, Component 2, Investment 1.3—D.D. 1243 2/8/2022, PE0000005).

Conflicts of Interest: The authors declare no conflicts of interest.

References

1. Ager, A. Improving the evaluation of spatial optimization models for prioritizing landscape restoration and wildfire risk reduction investments. *J. Environ. Manag.* **2024**, *360*, 121001. [CrossRef] [PubMed]
2. Russell, A.; Fontana, N.; Hoecker, T.; Kamanu, A.; Majumder, R.; Stephens, J.; Young, A.M.; Cravens, A.E.; Giardina, C.; Hiers, K.; et al. A fire-use decision model to improve the United States' wildfire management and support climate change adaptation. *Cell Rep. Sustain.* **2024**, *1*, 100125. [CrossRef]
3. Balik, J.A.; Coop, J.D.; Krawchuk, M.A.; Naficy, C.E.; Parisien, M.A.; Parks, S.A.; Stevens-Rumann, C.S.; Whitman, E. Biogeographic patterns of daily wildfire spread and extremes across North America. *Front. For. Glob. Change* **2024**, *7*, 1355361. [CrossRef]
4. Thompson, J.R.; Thomas, A. Spies, Vegetation and weather explain variation in crown damage within a large mixed-severity wildfire. *For. Ecol. Manag.* **2009**, *258*, 1684–1694. [CrossRef]
5. Bakhshaii, A.; Johnson, E.A. A review of a new generation of wildfire–atmosphere modeling. *Can. J. For. Res.* **2019**, *49*, 565–574. [CrossRef]
6. Tang, W.; He, C.; Emmons, L.; Zhang, J. Global expansion of wildland-urban interface (WUI) and WUI fires: Insights from a multiyear worldwide unified database (WUWUI). *Environ. Res. Lett.* **2024**, *19*, 044028. [CrossRef]

7. Ager, A.A.; Preisler, H.K.; Arca, B.; Spano, D.; Salis, M. Wildfire risk estimation in the Mediterranean area. *Environmetrics* **2014**, *25*, 384–396. [CrossRef]
8. Shive, K.L.; Sieg, C.H.; Fulé, P.Z. Pre-wildfire management treatments interact with fire severity to have lasting effects on post-wildfire vegetation response. *For. Ecol. Manag.* **2013**, *297*, 75–83. [CrossRef]
9. Valle Seijo, M.F.; Micheletti, M.I.; Otero, L.A.; Piacentini, R.D. Atmospheric pollutants in Rosario, Argentina analysed through remote sensing: Wildfires and COVID-19 lockdown effects. *Remote Sens. Appl. Soc. Environ.* **2024**, *36*, 101326. [CrossRef]
10. Bento-Gonçalves, A.; Vieira, A.; Santos, S.M.d. Research on Wildfires, Soil Erosion and Land Degradation in the XXI Century. *Fire* **2024**, *7*, 327. [CrossRef]
11. Borja, M.E.L.; Plaza-Álvarez, P.A.; Carmona Yáñez, M.D.; Miralles, I.; Ortega, R.; Soria, R.; Candel-Pérez, D.; Zema, D.A. Long-term evaluation of soil functionality in Mediterranean forests after a wildfire and post-fire hillslope stabilization. *For. Ecol. Manag.* **2024**, *555*, 121715. [CrossRef]
12. Abdollahi, M.; Vahedifard, F.; Leshchinsky, B.A. Hydromechanical modeling of evolving post-wildfire regional-scale landslide susceptibility. *Eng. Geol.* **2024**, *335*, 107538. [CrossRef]
13. Guiomar, N.; Godinho, S.; Fernandes, P.M.; Machado, R.; Neves, N.; Fernandes, J.P. Wildfire patterns and landscape changes in Mediterranean oak woodlands. *Sci. Total Environ.* **2015**, *536*, 338–352. [CrossRef] [PubMed]
14. Vogiatzoglou, K.; Papadimitriou, C.; Ampountolas, K.; Chatzimanolakis, M.; Koumoutsakos, P.; Bontozoglou, V. An interpretable wildfire spreading model for real-time predictions. *J. Comput. Sci.* **2024**, *83*, 102435. [CrossRef]
15. Liu, N. Wildland surface fire spread: Mechanism transformation and behavior transition. *Fire Saf. J.* **2023**, *141*, 103974. [CrossRef]
16. Bhatt, S.; Chouhan, U. An enhanced method for predicting and analysing forest fires using an attention-based CNN model. *J. For. Res.* **2024**, *35*, 67. [CrossRef]
17. Jain, P.; Coogan, S.C.P.; Subramanian, S.G.; Crowley, M.; Taylor, S.; Flannigan., M.D. A review of machine learning applications in wildfire science and management. *Environ. Rev.* **2020**, *28*, 478–505. [CrossRef]
18. Gonzalo, S.; Fuentes, A.; Valdivia, A.; Auat-Cheein, F.; Reszka, P. Assessing wildfire risk to critical infrastructure in central Chile: Application to an electrical substation. *International J. Wildland Fire* **2024**, *33*, WF22113. [CrossRef]
19. Arango, E.; Jiménez, P.; Nogal, M.; Sousa, H.S.; Steward, M.G.; Matos, J.C. Enhancing infrastructure resilience in wildfire management to face extreme events: Insights from the Iberian Peninsula. *Clim. Risk Manag.* **2024**, *44*, 100595. [CrossRef]
20. Ndalila, M.N.; Lala, F.; Makindi, S.M. Community perceptions on wildfires in Mount Kenya forest: Implications for fire preparedness and community wildfire management. *Fire Ecol.* **2024**, *20*, 92. [CrossRef]
21. Sun, Y.; Forrister, A.; Kuligowski, E.D.; Lovreglio, R.; Cova, T.J.; Zhao, X. Social vulnerabilities and wildfire evacuations: A case study of the 2019 Kincade fire. *Saf. Sci.* **2024**, *176*, 106557. [CrossRef]
22. Galiana-Martín, L. Spatial Planning Experiences for Vulnerability Reduction in the Wildland-Urban Interface in Mediterranean European Countries. *Eur. Countrys.* **2017**, *9*, 577–593. [CrossRef]
23. Elhami-Khorasani, N.; Ebrahimian, H.; Buja, L.; Cutter, S.L.; Kosovic, B.; Lareau, N.; Meacham, B.J.; Rowell, E.; Taciroglu, E.; Thompson, M.P.; et al. Conceptualizing a probabilistic risk and loss assessment framework for wildfires. *Nat. Hazards* **2022**, *114*, 1153–1169. [CrossRef]
24. Borisova, B.; Todorova, E.; Ihtimanski, I.; Glushkova, M.; Zhiyanski, M.; Georgieva, M.; Dimitrov, S. Wildfire risk assessment and mapping–an approach for Natura 2000 forest sites. Trees. *For. People* **2024**, *16*, 100532. [CrossRef]
25. Caron, N.; Guyeux, C.; Aynes, B. Predicting wildfire events with calibrated probabilities. In Proceedings of the 2024 16th International Conference on Machine Learning and Computing (ICMLC '24), Shenzhen, China, 2–5 February 2024; Association for Computing Machinery: New York, NY, USA, 2024; pp. 168–175. [CrossRef]
26. Liz-López, H.; Huertas-Tato, J.; Pérez-Aracil, J.; Casanova-Mateo, C.; Sanz-Justo, J.; Camacho, D. Spain on Fire: A novel wildfire risk assessment model based on image satellite processing and atmospheric information. *Knowl. Based Syst.* **2024**, *283*, 111198. [CrossRef]
27. Arima, S.; Calculli, C.; Pollice, A. A Zero-inflated Poisson spatial model with misreporting for wildfire occurrences in southern Italian municipalities. *Environmetrics* **2025**, *36*, e2853. [CrossRef]
28. Keeping, T.; Harrison, S.P.; Prentice, I.C. Modelling the daily probability of wildfire occurrence in the contiguous United States. *Environ. Res. Lett.* **2024**, *19*, 024036. [CrossRef]
29. Gonzalez-Mathiesen, C. Challenges in Developing Wildfire Understanding from Wildfire Information through Spatial Planning Processes. *Sustainability* **2024**, *16*, 420. [CrossRef]
30. Wei, G.; Qiu, F.; Liu, X. Convolutional Non-Homogeneous Poisson Process and its Application to Wildfire Ignition Risk Quantification for Power Delivery Networks. *Technometrics* **2024**, 1–19. [CrossRef]
31. Papakosta, P.; Straub, D. Probabilistic prediction of daily fire occurrence in the Mediterranean with readily available spatio-temporal data. *Iforest Biogeosci. For.* **2016**, *10*, 32. [CrossRef]
32. Services Dedicated to Municipalities: Fire Register. Geoportal of the Campania Region: Territorial Information System of the Campania Region. Available online: https://sit2.regione.campania.it/servizio/catasto-incendi (accessed on 10 July 2024).

33. AUTOCAD Software. Available online: https://www.autodesk.com/it/products/autocad/overview?term=1-YEAR&tab=subscription (accessed on 10 July 2024).
34. QGIS Software. Available online: http://qgis.osgeo.org (accessed on 10 July 2024).
35. Tarquini, S.; Isola, I.; Favalli, M.; Battistini, A.; Dotta, G. TINITALY, a Digital Elevation Model of Italy with a 10 Meters Cell Size (Version 1.1) National Institute of Geophysics and Volcanology (INGV) 2023. Available online: https://tinitaly.pi.ingv.it/ (accessed on 10 July 2024).
36. Bagnaia, R.; Viglietti, S.; Laureti, L.; Giacanelli, V.; Ceralli, D.; Bianco, P.M.; Loreto, A.; Luce, E.; Fusco, L. *Nature Map of the Campania Region: Habitat Map at a 1:25,000 Scale*; ISPRA: Campania, Italy, 2017.
37. Seitz, J.; Zhong, S.; Charney, J.J.; Heilman, W.E.; Clark, K.E.; Bian, X.; Skowronski, N.S.; Gallagher, M.R.; Patterson, M.; Cole, J.; et al. Atmospheric turbulence observed during a fuel-bed-scale low-intensity surface fire. *Atmos. Chem. Phys.* **2024**, *24*, 1119–1142. [CrossRef]
38. Finney, M.A.; Cohen, J.D.; McAllister, S.S.; Jolly, W.M. On the need for a theory of wildland fire spread. *Int. J. Wildland Fire* **2013**, *22*, 25–36. [CrossRef]
39. Bradley, D.R.; Bradley, T.D.; McGrath, S.G.; Cutcomb, S.D. Type I error rate of the chi-square test in independence in R × C tables that have small expected frequencies. *Psychol. Bull.* **1979**, *86*, 1290–1297. [CrossRef]
40. Berardi, D.; Galuppi, M.; Libertà, A.; Lombardi, M. Geostatistical Modeling of Wildfire Occurrence Probability: The Case Study of Monte Catillo Natural Reserve in Italy. *Fire* **2023**, *6*, 427. [CrossRef]
41. Lewis, D.; Burke, C.J. The use and misuse of the chi-square test. *Psychol. Bull.* **1949**, *46*, 433–489. [CrossRef]
42. Coogan Sean, C.P.; Xinli, C.; Piyush, J.; Flannigan, M.D. Seasonality and trends in human- and lightning-caused wildfires ≥ 2 ha in Canada, 1959–2018. *Int. J. Wildland Fire* **2020**, *29*, 473–485. [CrossRef]

Disclaimer/Publisher's Note: The statements, opinions and data contained in all publications are solely those of the individual author(s) and contributor(s) and not of MDPI and/or the editor(s). MDPI and/or the editor(s) disclaim responsibility for any injury to people or property resulting from any ideas, methods, instructions or products referred to in the content.